



Contents lists available at ScienceDirect

Bioorganic & Medicinal Chemistry

journal homepage: www.elsevier.com/locate/bmc

Synthesis and biological evaluation of 2,4-disubstituted phthalazinones as Aurora kinase inhibitors

Wei Wang^a, Xiu Feng^a, Huan-Xiang Liu^a, Shi-Wu Chen^{a,*}, Ling Hui^{b,c}

^a School of Pharmacy, Lanzhou University, Lanzhou 730000, China

^b Experimental Center of Medicine, General Hospital of Lanzhou Military Command, Lanzhou 730050, China

^c Key Laboratory of Stem Cells and Gene Drug of Gansu Province, General Hospital of Lanzhou Military Command, Lanzhou 730050, China

ARTICLE INFO

Article history:

Received 27 March 2018

Revised 20 April 2018

Accepted 21 April 2018

Available online xxxx

Keywords:

Aurora kinase

Antitumor

Phthalazinone

Cell cycle

ABSTRACT

A series of 2,4-disubstituted phthalazinones were synthesized and their biological activities, including antiproliferation, inhibition against Aurora kinases and cell cycle effects were evaluated. Among them, *N*-cyclohexyl-4-((4-(1-methyl-1*H*-pyrazol-4-yl)-1-oxophthalazin-2(1*H*)-yl) methyl) benzamide (**12c**) exhibited the most potent antiproliferation against five carcinoma cell lines (HeLa, A549, HepG2, LoVo and HCT116 cells) with IC₅₀ values in range of 2.2–4.6 μM, while the IC₅₀ value of reference compound VX-680 was 8.5–15.3 μM. Moreover, Aurora kinase assays exhibited that compound **12c** was potent inhibitor of AurA and AurB kinase with the IC₅₀ values were 118 ± 8.1 and 80 ± 4.2 nM, respectively. Molecular docking studies indicated that compound **12c** forms better interaction with both AurA and AurB. Furthermore, compound **12c** induced G2/M cell cycle arrest in HeLa cells by regulating protein levels of cyclinB1 and cdc2. These results suggested that **12c** is a promising pan-Aurora kinase inhibitor for the potential treatment of cancer.

© 2018 Elsevier Ltd. All rights reserved.

1. Introduction

Mitotic kinases play an essential role in mitosis, Aurora and other mitotic kinases are often observed over-expression in human solid and many hematologic cancers.¹ As one of serine/threonine kinases, Aurora kinase family is involved in centrosome maturation, mitotic spindle formation, chromosome segregation and cytokinesis during mitosis.^{2,3} The family includes three kinases designated as Aurora A (AurA), B (AurB) and C (AurC), which possess a carboxy-terminal catalytic domain and an amino-terminal regulatory domain^{4–7} However, these kinases have quite different and nonoverlapping functions in mitotic processes.⁸ AurA increases during late G2 to M phase, and it is involved in centrosome maturation, centrosome separation, bipolar-spindle assembly and other mitotic events^{9–11} AurB is located at chromosome 17p13.1, and it is essential for chromosome segregation and execution of cytokinesis.¹² AurC is a chromosomal passenger protein, which appears to have overlapping functions with AurB during mitotic cell division process.¹³

Aurora kinases have become a promising anticancer targets since they are related to oncogenesis and tumor progression, and many small molecule Aurora kinases inhibitors have been devel-

oped including VX-680, AT9283, AZD1152 and AMG900 (Fig. 1).¹⁴ VX-680 is the first generation of Aurora kinase inhibitor, which blocks cell-cycle progression and induces apoptosis in human tumor. Crystal structure for VX-680 in complex with Aurora kinases show that it occupies the ATP-binding site in Aurora kinases to inhibit catalytic activity.^{15,16} AT9283 is a benzimidazole derivative, which suppresses growth and survival in HCT116 cells and produced the polyploid phenotype by inhibiting AurB kinase.¹⁷ AZD1152, a quinazoline derivative, is a selective inhibitor of AurB kinase and displays striking activity *in vivo*.¹⁸ AMG900 is potent pan-Aurora kinase inhibitor, which belongs to phthalazine derivative. It inhibits autophosphorylation of AurA and pHisH3 on Ser10 *in vitro* and suppresses the growth of human tumor xenografts *in vivo*.¹⁹

Phthalazinones exhibited broad activities, such as antihypertensive,²⁰ antifungal effect,²¹ Histamine H1 receptor antagonist²² and bradykinin B1 receptor antagonist.²³ Prime et al. replaced phthalazine with phthalazinone scaffolds and found phthalazinone is an important pharmacology core for Aurora kinases.²⁴ Compound **1** is a phthalazinone derivative and the crystal structure for **1** in complex with Aurora kinases show that the amino-pyrazole of **1** can form hydrogen bounds with the hinge region of Aurora A, and the benzyl of **1** may form hydrophobic interaction with Aurora kinases.²⁴ However, basis on crystal structure analysis, we considered that the benzyl of **1** was too small to completely occupy the

* Corresponding author.

E-mail address: chenshw@lzu.edu.cn (S.-W. Chen).

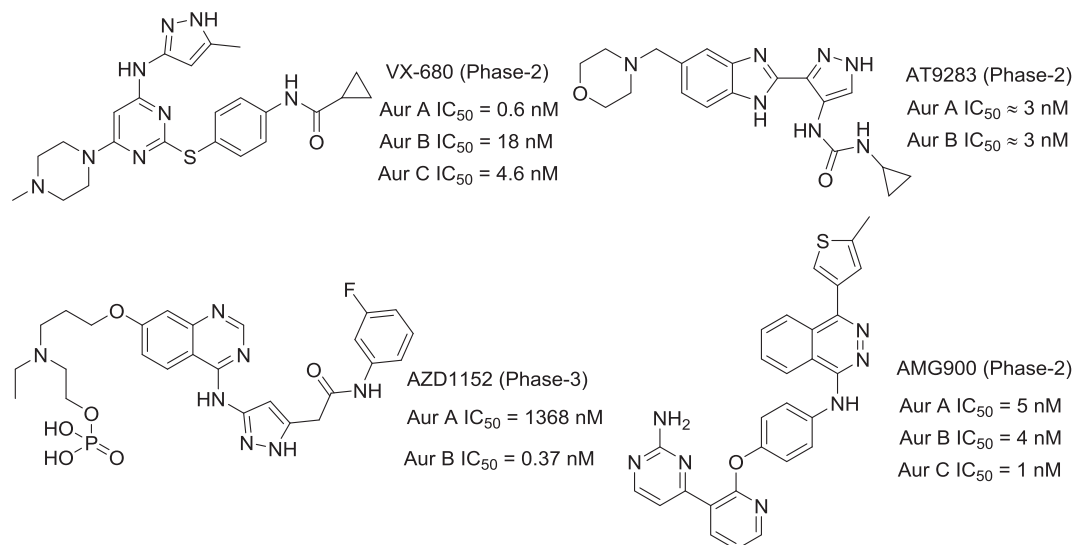


Fig. 1. Some Aurora kinase inhibitors in clinical trials.

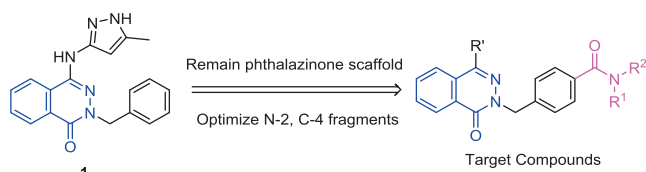


Fig. 2. The design of target compounds derived from 1.

hydrophobic pocket of Aurora kinases, which might accommodate a larger group. Herein, we designed and synthesized a series of 2,4-disubstituted phthalazinones (Fig. 2) by optimizing N-2 and C-4 fragments as Aurora kinase inhibitors, and evaluated their activities in human tumor cell lines.

2. Results and discussion

2.1. Chemistry

Intermediates **3a-g** were easily obtained through reaction of 4-(chloromethyl) benzoic acid (**2**) with corresponding amine, under 1-(3-dimethylaminopropyl)-3-ethylcarbodiimide hydrochloride (EDCI) in the presence of *N*-hydroxybenzotriazole (HOBT) in dichloromethane at room temperature.²⁵ Simultaneously, treatment of 4-nitrobenzoyl chloride (**4**) with morpholine or 2-chloroaniline afforded **5a-b**. **5a-b** were reduced to provide 4-amino-benzamides **6a-b** (Scheme 1).²⁶

The general synthesis of the initial phthalazinone analogues starts from phthalic anhydride and is outlined in Scheme 2. First, hydrazine insertion into phthalic anhydride affords phthalazine-1,4-dione (**7**) in quantitative yield. Subsequent dibromination followed by monohydrolysis gives the desired bromophthalazinone (**9**) in good yield.²⁴ Subsequent treatment of **9** with **3a-g** in dimethylformamide (DMF) in the presence of NaH at room temperature to get intermediates **10a-g**. Finally, **10a-g** were reacted with 3,5-dimethylisoxazole-4-boronic acid or 1-methyl-4-(4,4,5,5-tetramethyl-1,3,2-dioxaborolan-2-yl)-1*H*-pyrazole via palladium-catalyzed Suzuki coupling reaction to produce target compounds **11a-g** or **12a-g**. Simultaneously, **10c** were reacted with 1-methyl-1*H*-pyrazol-4-amine or **6a-b** via palladium-catalyzed Buchwald-Hartwig coupling to produce target compounds **13a-c**.²⁷ The newly synthesized compounds **11a-g**, **12a-g** and **13a-c**

were characterized by physicochemical and spectral means, and both analytical and spectral data of all the compounds were in full agreement with the proposed structures.

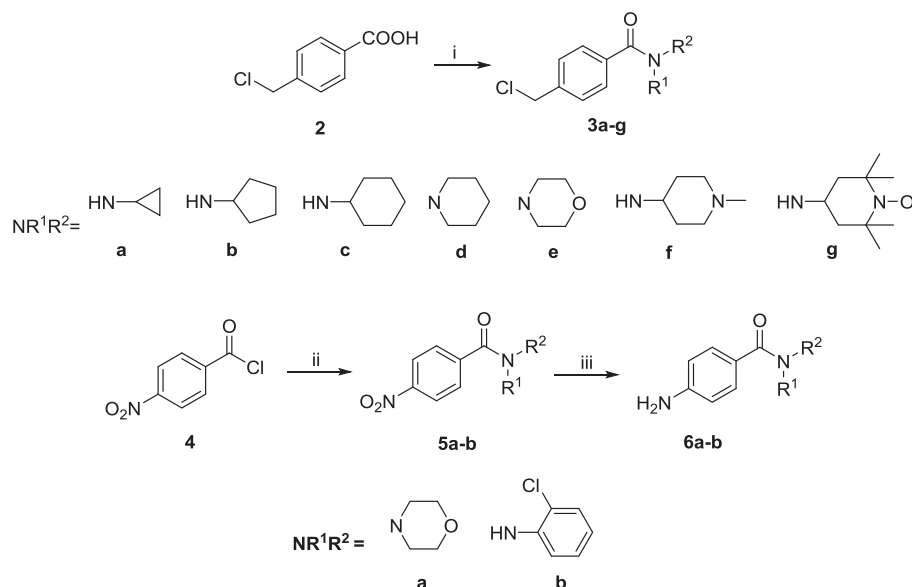
2.2. Biology

2.2.1. Antiproliferation activities of target compounds

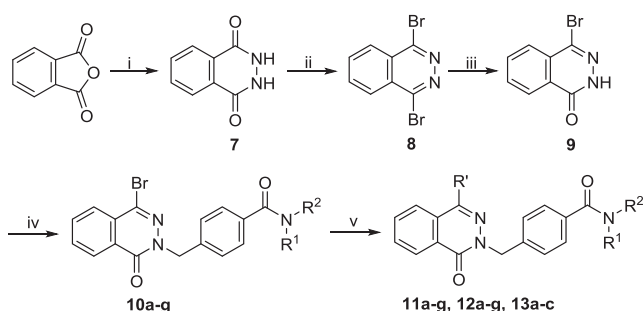
The antiproliferation activities of target compounds **11a-g**, **12a-g** and **13a-c** were screened against five human tumor cell lines (HeLa, A549, HepG2, LoVo and HCT116) by MTT assay after treatment for 72 h, with **1** and VX-680 as reference compounds.²⁸ As shown in Table 1, some target compounds showed better or equivalent antiproliferation activity in five human tumor cell lines compared with VX-680 and **1**. Furthermore, compounds **12a-g** with the 1-methyl-1*H*-pyrazole chain at the C-4 position showed more potent antiproliferation activity than those of compounds **11a-g** with the 3,5-dimethylisoxazole chain in these five human tumor cell lines. And compounds **13b-c** displayed significantly reduce as well as **13a** showed the slightly decrease compared with **12c** in their *in vitro* antiproliferation activities, suggesting that the 1-methyl-1*H*-pyrazole group at the 4-position of phthalazinone plays a crucial role in maintaining the antiproliferative activities. In addition, the antiproliferation activities of compounds **12a-c** were successively increasing with the increasing of amine substituent size of 4-methylbenzamide at 2-position of phthalazinone. Among the synthetic target compounds, compound **12c** showed the strongest growth-inhibitory activities in the five human tumor cell lines with the IC₅₀ values were 2.2 ± 0.2, 3.3 ± 0.5, 4.6 ± 0.7, 2.6 ± 0.3 and 3.8 ± 0.3 μM for the HeLa, A549, HepG2, LoVo and HCT116 tumor cell lines, respectively.

2.2.2. Aurora kinases inhibitory activities of the selected compounds

Next, compounds **12b**, **12c**, **12f**, **12g** and **13a** were selected to identify the inhibition activities against Aurora kinases by Kinase-Glo luminescent kinase assay *in vitro*,²⁹ with VX-680 as reference compound. As showed in Table 2, compound **12c** exhibited the most potent inhibition on AurA and AurB with the IC₅₀ values were 118 ± 8.1 and 80 ± 4.2 nM, respectively. The other compounds showed slightly less inhibition activities against AurA and AurB. Aurora kinases inhibition results of those compounds were consistent with antiproliferative activity, suggesting that those compounds inhibit cancer cell proliferation by targeting Aurora kinases.



Scheme 1. Reagents and conditions: (i) amine, EDCI, HOBT, DCM, rt; (ii) amine, triethylamine, CH_2Cl_2 , 0 °C; (iii) NH_4Cl , Fe, ethanol: $\text{H}_2\text{O} = 4:1$, 80 °C.



Scheme 2. Reagents and conditions: (i) hydrazine, AcOH, 120 °C; (ii) POBr_3 , DCE, reflux; (iii) AcOH, 120 °C; (iv) **3a-g**, NaH, DMF, rt; (v) a) 3,5-Dimethylisoxazole-4-boronic acid (for **11a-g**), $\text{Pd}(\text{dppf})_2\text{Cl}_2$, Na_2CO_3 , H_2O -dioxane, N_2 , reflux; b) 1-Methyl-4-(4,4,5,5-tetramethyl-1,3,2-dioxaborolan-2-yl)-1H-pyrazole (for **12a-g**), $\text{Pd}(\text{dppf})_2\text{Cl}_2$, Na_2CO_3 , H_2O -dioxane, N_2 , reflux; c) 1-methyl-1H-pyrazol-4-amine or **6a-b** (for **13a-c** from **10c**), Pd_2dba_3 , 2-(di-*tert*-butylphosphino)biphenyl, *t*-BuOK, toluene, N_2 , reflux.

2.2.3. Compound **12c** blocks Aurora kinases phosphorylation in HeLa cells

AurA is activated by phosphorylation of Thr288, and AurB is activated by phosphorylation of Thr232^{30–32}. To further identify the Aurora kinases as targets of compound **12c**, the phosphorylation of AurA on Thr288 and AurB on Thr232 were investigated in HeLa cells treated with various concentrations of compound **12c** (0, 0.5, 2.5 and 5.0 μM) for 6 h by western blot.³³ As shown in Fig. 3, compound **12c** obviously decreased phosphorylation of AurA on Thr288, and reduced phosphorylation of AurB on Thr232 in a dose-dependent manner. These results suggested that compound **12c** is a potential Aurora kinases inhibitor although its potency was slightly weaker than that of VX-680.

2.2.4. Aurora kinases binding model of compound **12c**

To gain insight into the interaction of compound **12c** with AurA (PDB code: 3D14) and AurB (PDB code: 4C2V), docking simulation was performed using Glide module (Glide, version 6.7, Schrödinger, LLC, New York, NY, 2015) of Schrödinger software (Maestro, version 10.1, Schrödinger, LLC, New York, NY, 2015).³⁴ All the figures displaying the docking results were obtained using the scientific software Pymol.³⁵ The overview of the binding site of **12c** is

shown in Fig. 4. For AurA (Fig. 4A), the amine group at C2 of **12c** can form hydrogen bond with Asp287. For AurB (Fig. 4B), compound **12c** can form hydrogen bond with Ala173. As shown in Fig. 4C and D, the *N*-cyclohexyl-4-methylbenzamide moiety of **12c** can better occupy the hydrophobic pocket of AurA and AurB than that of compound **1**. The model would also be helpful for us to further understand the phthalazinone analogues were potent Aurora kinases inhibitors.

2.2.5. Compound **12c** induces cell cycle arrest in G2/M phase

The Aurora inhibitors including VX-680 often induce cancer cells cycle arrest in the G2/M phase.³⁶ Therefore, we also investigated the effects of **12c** on cell-cycle progression using fluorescence-activated cell sorting analysis of propidium iodide-stained HeLa cells.²⁵ As shown in Fig. 5, treatment with **12c** resulted in a dose-dependent accumulation of cells in the G2/M phase with a concomitant decrease in the population of G1 phase cells. Exposure to 0.5 and 5.0 μM of compound **12c** for 24 h, the percentages of cells in G2/M phase arrest were 34.66% and 87.17%, respectively, compared with 9.63% in untreated cultures.

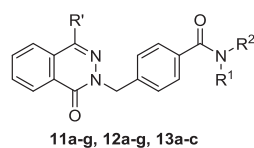
2.2.6. Compound **12c** reduces expression of cyclinB1 and cdc2

In eukaryotic cells, progression of cells from the G2 phase to M phase is triggered by activation of the cyclinB1-dependent cdc2 kinase.³⁷ As key regulators of the cell cycle, cyclinB1 and cdc2 are regulated by several complex mechanisms. Therefore, we used western blot to measure protein expression levels of cyclinB1 and cdc2 in HeLa cells following treatment with compound **12c** (0, 0.5, 2.0 and 5.0 μM) for 24 h, VX-680 as reference compound.³⁸ As shown in Fig. 6, with increasing concentration of **12c**, a marked decrease in cyclinB1 and cdc2 protein levels compared with the control and VX-680 were observed, suggesting that **12c** influenced the protein expression levels of cyclinB1 and cdc2 and hence promote cell-cycle arrest in the G2/M phase.

3. Conclusions

In summary, we described a series of 2,4-disubstituted phthalazinones small molecule inhibitors that showed potent cytotoxicity against the human tumor cell lines. Furthermore, we specifically

Table 1
The cytotoxicities of compounds **11a-g**, **12a-g** and **13a-c**.



Compds	NR ¹ R ²	R'	(IC ₅₀ , μM) ^a				
			HeLa ^b	A549 ^b	HepG2 ^b	LoVo ^b	HCT116 ^b
11a			> 100	> 100	> 100	> 100	> 100
11b			> 100	> 100	> 100	> 100	> 100
11c			> 100	> 100	> 100	82.2 ± 4.8	> 100
11d			> 100	86.2 ± 4.3	97.3 ± 5.6	> 100	> 100
11e			> 100	> 100	> 100	84.4 ± 5.6	> 100
11f			> 100	> 100	> 100	> 100	84.9 ± 7.3
11g			83.5 ± 4.9	84.3 ± 8.4	85.1 ± 6.4	41.2 ± 7.3	36.8 ± 4.3
12a			40.0 ± 2.6	51.2 ± 3.4	> 100	48.2 ± 5.1	20.1 ± 5.3
12b			16.7 ± 3.7	32.3 ± 6.2	84.3 ± 6.8	23.7 ± 4.2	14.3 ± 2.4
12c			2.2 ± 0.2	3.3 ± 0.5	4.6 ± 0.7	2.6 ± 0.3	3.8 ± 0.3
12d			65.5 ± 3.2	67.4 ± 2.7	73.1 ± 4.5	77.1 ± 7.3	73.9 ± 5.7
12e			> 100	73.3 ± 5.4	> 100	52.3 ± 6.3	> 100
12f			28.5 ± 4.3	54.3 ± 5.9	47.3 ± 3.8	83.3 ± 6.4	69.5 ± 5.3
12g			27.7 ± 2.2	37.3 ± 3.6	27.4 ± 2.9	50.1 ± 6.1	50.5 ± 4.3
13a			3.2 ± 0.2	6.8 ± 0.6	8.3 ± 0.5	5.3 ± 0.2	5.4 ± 0.3
13b			23.2 ± 2.4	64.3 ± 2.5	40.4 ± 5.2	54.5 ± 7.3	48.2 ± 4.3
13c			87.3 ± 4.6	> 100	82.4 ± 3.4	79.5 ± 4.5	> 100
1	–	–	6.3 ± 0.6	42.6 ± 2.3	11.3 ± 0.9	22.2 ± 2.2	22.7 ± 1.1
VX680	–	–	8.5 ± 2.1	15.3 ± 3.2	13.7 ± 2.4	12.4 ± 1.5	10.1 ± 1.3

^a IC₅₀ values are presented as the means ± SD of triplicate experiments.

^b MTT method drug exposure for 72 h.

found that compound **12c** inhibited Aurora kinases by decreasing phosphorylation of AurA on Thr288 and AurB on Thr232. Additionally, treatment with compound **12c** also resulted G2/M accumulation via the cell-cycle regulators cyclin B1 and cdc2 in HeLa cells. Taken together, compound **12c** is a potential anticancer agent by targeting Aurora kinase.

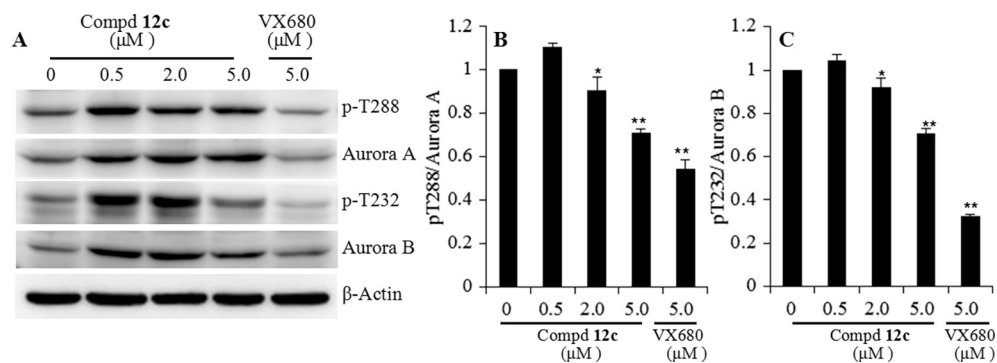
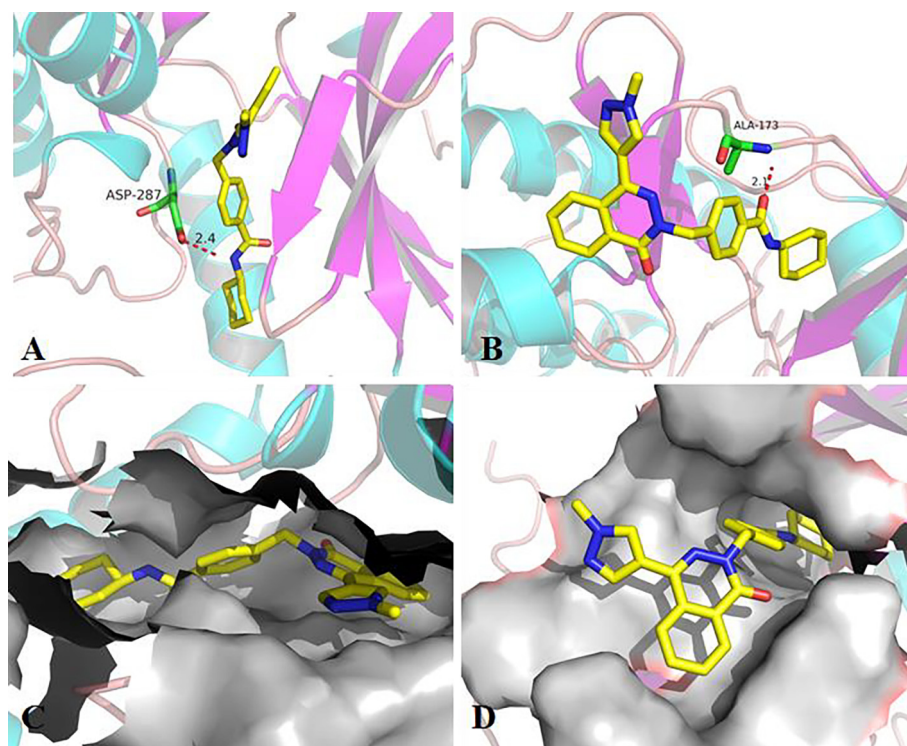
4. Experiment

4.1. Chemistry

All starting materials and reagents were purchased commercially and used without further purified, unless otherwise stated. All

Table 2The kinase inhibitions of selected compounds *in vitro*.

Compds	(IC ₅₀ , nM) ^a		Compds	(IC ₅₀ , nM) ^a	
	Aurora A	Aurora B		Aurora A	Aurora B
12b	583 ± 15.3	265 ± 11.5	12g	168 ± 12.4	134 ± 13.2
12c	118 ± 8.1	80 ± 4.2	13a	145 ± 7.4	132 ± 6.1
12f	183 ± 6.1	105 ± 7.3	VX-680	1 ± 0.2	15 ± 1.4

^a The IC₅₀ values are the means of at least two experiments.**Fig. 3.** Western blot for inhibition of p-T288, AurA, p-T232 and AurB with various concentrations of compound **12c** in HeLa cells for 6 h. The results are expressed as the mean ± SD; *P < 0.05, **P < 0.001 versus control.**Fig. 4.** The binding mode of **12c** with AurA (PDB code: 3D14) and AurB (PDB code: 4C2V). (A) The interaction between **12c** and AurA. (B) The interaction between **12c** and AurB. (C) The binding pocket of AurA was shown in surface. (D) The binding pocket of AurB was shown in surface. The surface is colored by gray.

reactions were monitored by thin layer chromatograph (TLC) on silica gel GF254 (0.25 mm thick). Column chromatography (CC) was performed on Silica Gel 60 (230–400 mesh, Qingdao Ocean Chemical Ltd., China). ¹H NMR and ¹³C NMR spectra were recorded with a Agilent NMR inova 600 spectrometer with TMS as an internal standard, all chemical shift values are reported as ppm. Mass spectra were recorded on a Bruker Dalton APEXII49e and Esquire 6000 (ESI-ION TRAP) spectrometer with ESI source as ionization,

respectively. Melting points were determined in Kofler apparatus and were uncorrected. EPR signals were obtained on a Bruker A300-9.5/12 spectrometer.

4.1.1. Procedures for synthesis of **3a-g**

4.1.1.1. 4-(Chloromethyl)-N-cyclopropylbenzamide (**3a**). A mixture of 4-(chloromethyl)benzoic acid (**2**) (1.0 g, 5.9 mmol), cyclopropanamine (0.824 g/mL, 5.9 mmol), EDCI (7.1 mmol) and HOBT

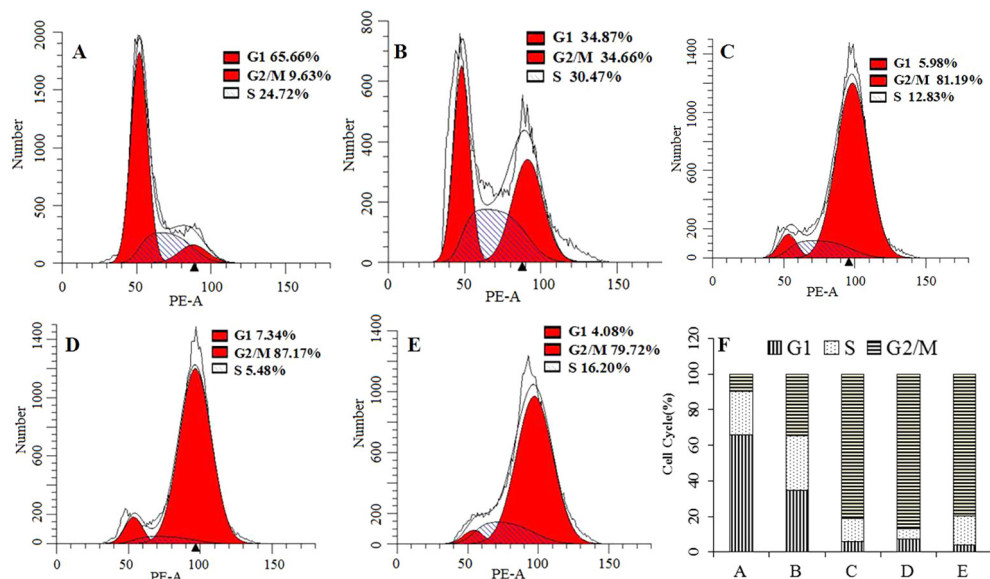


Fig. 5. Effect of **12c** on cell cycle progression. (A) Control HeLa cells; (B) HeLa cells treated with 0.5 μM **12c** for 24 h; (C) HeLa cells treated with 2.0 μM **12c** for 24 h; (D) HeLa cells treated with 5.0 μM **12c** for 24 h; (E) HeLa cells treated with 5.0 μM VX680 for 24 h; (F) Bar graphs showing compound **12c** on cell cycle progression.

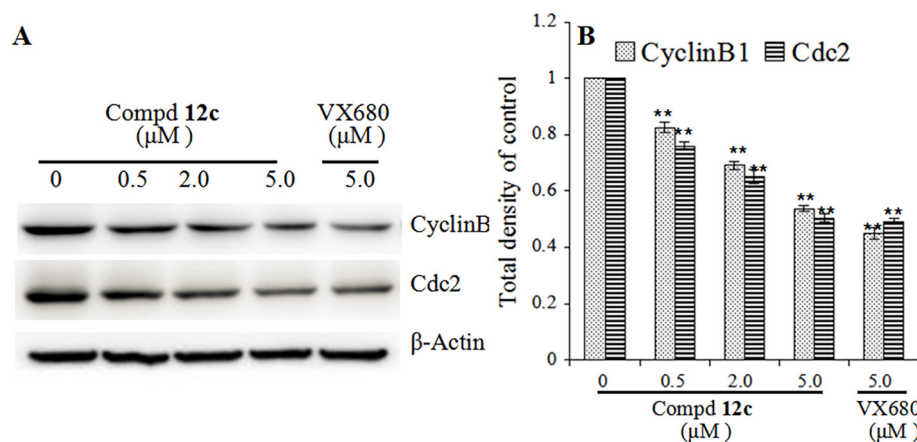


Fig. 6. Western blot analysis of expression of cyclinB1 and cdc2 in HeLa cells treated with **12c** (0, 0.5, 2.0 and 5.0 μM) or VX-680 (5.0 μM) for 24 h. The results are expressed as the mean ± SD; *P < 0.05, **P < 0.001 versus control.

(7.1 mmol) was stirred in anhydrous DCM (20 mL) for 6 h at room temperature. After the reaction was finished, the mixture was filtered and filtrate was evaporated in vacuo, the crude product was further purified by column chromatography on silica gel to yield compound **3a** (92%) as a white solid. $^1\text{H NMR}$ (600 MHz, CDCl_3) δ 7.73 (d, $J = 8.4$ Hz, 2H), 7.44 (d, $J = 8.4$ Hz, 2H), 6.24 (s, 1H), 4.60 (s, 2H), 2.90 (q, $J = 3.6$ Hz, 1H), 0.90–0.86 (m, 2H), 0.64–0.60 (m, 2H).

4.1.1.2. 4-(Chloromethyl)-N-cyclopentylbenzamide (3b). With cyclopentanamine, a similar procedure as that described for **3a** gave pure **3b** (90%) as a white solid. $^1\text{H NMR}$ (600 MHz, CDCl_3) δ 7.74 (d, $J = 7.8$ Hz, 2H), 7.45 (d, $J = 8.4$ Hz, 2H), 6.24 (t, $J = 1.8$ Hz, 1H), 4.61 (s, 2H), 2.90 (q, $J = 7.2$ Hz, 1H), 2.12–2.07 (m, 2H), 1.75–1.65 (m, 4H), 1.49 (q, $J = 6.6$ Hz, 2H).

4.1.1.3. 4-(Chloromethyl)-N-cyclohexylbenzamide (3c). With cyclohexanamine, a similar procedure as that described for **3a** gave pure **3c** (93%) as a white solid. $^1\text{H NMR}$ (600 MHz, CDCl_3) δ 7.74 (d, $J = 8.4$ Hz, 2H), 7.44 (d, $J = 8.4$ Hz, 2H), 5.96 (s, 1H), 4.60 (s, 2H), 2.90

(q, $J = 4.2$ Hz, 1H), 2.04–2.00 (m, 2H), 1.77–1.72 (m, 2H), 1.68–1.63 (m, 1H), 1.47–1.38 (m, 2H), 1.28–1.18 (m, 3H).

4.1.1.4. (4-(Chloromethyl)phenyl)(piperidin-1-yl)methanone (3d). With piperidine, a similar procedure as that described for **3a** gave pure **3d** (88%) as a white solid. $^1\text{H NMR}$ (600 MHz, CDCl_3) δ 7.42 (d, $J = 7.8$ Hz, 2H), 7.38 (d, $J = 8.4$ Hz, 2H), 4.60 (s, 2H), 3.71 (brs, 2H), 3.33 (brs, 2H), 1.68 (brs, 4H), 1.52 (brs, 2H).

4.1.1.5. (4-(Chloromethyl)phenyl)(morpholino)methanone (3e). With morpholine, a similar procedure as that described for **3a** gave pure **3e** (89%) as a white solid. $^1\text{H NMR}$ (600 MHz, CDCl_3) δ 7.44 (d, $J = 8.4$ Hz, 2H), 7.41 (d, $J = 7.8$ Hz, 2H), 4.60 (s, 2H), 3.84–3.40 (m, 8H).

4.1.1.6. 4-(Chloromethyl)-N-(1-methylpiperidin-4-yl)benzamide (3f). With 1-methylpiperidin-4-amine, a similar procedure as that described for **3a** gave pure **3f** (70%) as a white solid. $^1\text{H NMR}$ (600 MHz, $\text{DMSO-}d_6$) δ 8.26 (d, $J = 7.8$ Hz, 1H), 7.83 (d, $J = 7.2$ Hz, 2H), 7.50 (d, $J = 8.4$ Hz, 2H), 4.81 (s, 2H), 3.72 (q, $J = 3.6$ Hz, 1H), 2.77 (d, $J = 10.8$ Hz, 2H), 2.17 (s, 3H), 1.96 (t, $J = 10.8$ Hz, 2H), 1.75 (d, $J = 11.4$ Hz, 2H), 1.61–1.55 (m, 2H).

4.1.1.7. 4-(Chloromethyl)-N-[(2,2,6,6-tetramethyl-1-oxyl)piperidin-4-yl]benzamide (**3g**). With 4-NH₂-TEMPO, a similar procedure as that described for **3a** gave pure **3g** (90%) as a pink solid. ¹H NMR (600 MHz, CDCl₃) (**3g** is a free-radical, some signals appear broadened and other signals are missing) δ 7.77 (brs, 2H), 7.50 (s, 2H), 4.62 (s, 2H). MS (ESI) *m/z* 325.1 ([M+2H]⁺).

4.1.2. Procedures for synthesis of **5a–b** and **6a–b**

4.1.2.1. Morpholino(4-nitrophenyl)methanone (**5a**). To a stirred solution of 4-nitrobenzoyl chloride (**4**) (11.8 mmol) and triethylamine (11.8 mmol) in 15 mL dry CH₂Cl₂ at 0 °C was dropwise added dichloromethane solution of morpholine (14.2 mmol), and then the the temperature of the mixture warmed to room temperature naturally. After stirring for 24 h, the reaction mixture was concentrated under reduced pressure gave the crude product **5a** (91%) as a yellow solid. ¹H NMR (600 MHz, CDCl₃) δ 8.30 (d, *J* = 7.8 Hz, 2H), 7.59 (d, *J* = 8.4 Hz, 2H), 3.83–3.38 (m, 8H).

4.1.2.2. N-(2-Chlorophenyl)-4-nitrobenzamide (**5b**). With 2-chloroaniline, a similar procedure as that described for **5a** gave pure **5b** (90%) as a yellow solid. ¹H NMR (600 MHz, CDCl₃) δ 8.52 (d, *J* = 8.4 Hz, 1H), 8.44 (s, 1H, NH), 8.38 (d, *J* = 8.4 Hz, 2H), 8.09 (d, *J* = 8.4 Hz, 2H), 7.45 (d, *J* = 7.2 Hz, 1H), 7.39–7.35 (m, 1H), 7.17–7.13 (m, 1H).

4.1.2.3. (4-Aminophenyl)(morpholino)methanone (**6a**). A solution of morpholino(4-nitrophenyl)methanone (**5a**) (6.3 mmol) with NH₄Cl (6.3 mmol) and Fe (31.5 mmol) in 4:1 ethanol:H₂O (100 mL) was heated at 80 °C for 3 h. After the mixture was cooled, the solvent was evaporated and the residue was purified by column chromatography on silica gel to yield compound **6a** (82%) as a white solid. ¹H NMR (600 MHz, CDCl₃) δ 7.26 (d, *J* = 8.4 Hz, 2H), 6.65 (d, *J* = 8.4 Hz, 2H), 3.89 (s, 2H, NH₂), 3.70–3.64 (m, 8H).

4.1.2.4. 4-Amino-N-(2-chlorophenyl)benzamide (**6b**). With compound **5b**, a similar procedure as that described for **6a** gave pure **6b** (80%) as a white solid. ¹H NMR (600 MHz, CDCl₃) δ 8.56 (d, *J* = 9.0 Hz, 1H), 8.35 (s, 1H, NH), 7.76 (d, *J* = 8.4 Hz, 2H), 7.40 (d, *J* = 8.4 Hz, 1H), 7.32 (t, *J* = 7.8 Hz, 1H), 7.05 (t, *J* = 7.8 Hz, 1H), 6.73 (d, *J* = 7.8 Hz, 2H), 4.11 (s, 2H, NH₂).

4.1.3. Procedures for synthesis of **10a–g**

4.1.3.1. 4-((4-Bromo-1-oxophthalazin-2(1H)-yl)methyl)-N-cyclopropylbenzamide (**10a**). 4-Bromophthalazin-1(2H)-one (**9**) (1.3 mmol) and NaH (1.3 mmol) were dissolved in anhydrous DMF and stirred for 30 min at room temperature, then added 4-(chloromethyl)-N-cyclopropylbenzamide (**3a**) (1.0 mmol) into reaction mixture. After stirring for 48 h, concentration of the reaction mixture under reduced pressure gave the crude product was further purified by column chromatography on silica gel to yield compound **10a** (62%) as a white solid. ¹H NMR (600 MHz, CDCl₃) δ 8.42 (d, *J* = 8.4 Hz, 1H), 7.95 (d, *J* = 7.2 Hz, 1H), 7.88 (t, *J* = 7.2 Hz, 1H), 7.82 (t, *J* = 7.2 Hz, 1H), 7.69 (d, *J* = 8.4 Hz, 2H), 7.51 (d, *J* = 7.8 Hz, 2H), 6.19 (s, 1H, NH), 5.39 (s, 2H), 2.89–2.87 (m, 1H), 0.87–0.84 (m, 2H), 0.62–0.57 (m, 2H).

4.1.3.2. 4-((4-Bromo-1-oxophthalazin-2(1H)-yl)methyl)-N-cyclopentylbenzamide (**10b**). With **3b**, a similar procedure as that described for **10a** gave pure **10b** (60%) as a white solid. ¹H NMR (600 MHz, CDCl₃) δ 8.43 (d, *J* = 7.8 Hz, 1H), 7.95 (d, *J* = 7.2 Hz, 1H), 7.88 (t, *J* = 7.2 Hz, 1H), 7.82 (t, *J* = 7.2 Hz, 1H), 7.70 (d, *J* = 7.8 Hz, 2H), 7.52 (d, *J* = 8.4 Hz, 2H), 5.98 (d, *J* = 7.8 Hz, 1H, NH), 5.40 (s, 2H), 4.38 (q, *J* = 7.2 Hz, 1H), 2.10–2.04 (m, 2H), 1.73–1.63 (m, 4H), 1.60–1.43 (m, 2H).

4.1.3.3. 4-((4-Bromo-1-oxophthalazin-2(1H)-yl)methyl)-N-cyclohexylbenzamide (**10c**). With **3c**, a similar procedure as that

described for **10a** gave pure **10c** (68%) as a white solid. ¹H NMR (600 MHz, CDCl₃) δ 8.42 (d, *J* = 7.8 Hz, 1H), 7.95 (d, *J* = 7.8 Hz, 1H), 7.88 (t, *J* = 7.2 Hz, 1H), 7.82 (t, *J* = 7.2 Hz, 1H), 7.71 (d, *J* = 7.8 Hz, 2H), 7.52 (d, *J* = 8.4 Hz, 2H), 5.90 (d, *J* = 7.8 Hz, 1H, NH), 5.40 (s, 2H), 3.95 (t, *J* = 4.2 Hz, 1H), 2.00 (d, *J* = 10.2 Hz, 2H), 1.73 (d, *J* = 13.2 Hz, 2H), 1.64 (d, *J* = 12.6 Hz, 1H), 1.45–1.37 (m, 2H), 1.26–1.17 (m, 3H).

4.1.3.4. 4-Bromo-2-(4-(piperidine-1-carbonyl)benzyl)phthalazin-1(2H)-one (**10d**). With **3d**, a similar procedure as that described for **10a** gave pure **10d** (63%) as a white solid. ¹H NMR (600 MHz, CDCl₃) δ 8.43 (d, *J* = 7.8 Hz, 1H), 7.96 (d, *J* = 7.2 Hz, 1H), 7.88 (t, *J* = 7.8 Hz, 1H), 7.82 (t, *J* = 8.4 Hz, 1H), 7.51 (d, *J* = 7.8 Hz, 2H), 7.36 (d, *J* = 7.8 Hz, 2H), 5.38 (s, 2H), 3.68 (brs, 2H), 3.31 (brs, 2H), 1.66–1.45 (m, 6H).

4.1.3.5. 4-Bromo-2-(4-(morpholine-4-carbonyl)benzyl)phthalazin-1(2H)-one (**10e**). With **3e**, a similar procedure as that described for **10a** gave pure **10e** (65%) as a white solid. ¹H NMR (600 MHz, CDCl₃) δ 8.43 (d, *J* = 7.8 Hz, 1H), 7.96 (d, *J* = 7.2 Hz, 1H), 7.88 (t, *J* = 7.2 Hz, 1H), 7.82 (t, *J* = 7.8 Hz, 1H), 7.53 (d, *J* = 7.8 Hz, 2H), 7.38 (d, *J* = 7.2 Hz, 2H), 5.39 (s, 2H), 3.76–3.40 (m, 8H).

4.1.3.6. 4-((4-Bromo-1-oxophthalazin-2(1H)-yl)methyl)-N-(1-methylpiperidin-4-yl)benzamide (**10f**). With **3f**, a similar procedure as that described for **10a** gave pure **10f** (54%) as a white solid. ¹H NMR (600 MHz, DMSO *d*₆) δ 8.33 (d, *J* = 7.8 Hz, 1H), 8.25 (d, *J* = 7.2 Hz, 1H), 8.07 (t, *J* = 7.2 Hz, 1H), 8.00–7.96 (m, 2H), 7.80 (d, *J* = 8.4 Hz, 2H), 7.40 (d, *J* = 8.4 Hz, 2H), 5.37 (s, 2H), 3.78 (d, *J* = 6.0 Hz, 1H), 2.90 (d, *J* = 6.0 Hz, 2H), 2.29 (s, 3H), 2.20 (brs, 2H), 1.79 (d, *J* = 11.4 Hz, 2H), 1.66–1.60 (m, 2H).

4.1.3.7. 4-((4-Bromo-1-oxophthalazin-2(1H)-yl)methyl)-N-[(2,2,6,6-tetramethyl-1-oxyl)piperidin-4-yl]benzamide (**10g**). With **3g**, a similar procedure as that described for **10a** gave pure **10g** (58%) as a pink solid. ¹H NMR (600 MHz, CDCl₃) (**10g** is a free-radical, some signals appear broadened and other signals are missing) δ 8.43 (d, *J* = 7.8 Hz, 1H), 7.76 (d, *J* = 7.8 Hz, 1H), 7.89 (t, *J* = 7.8 Hz, 1H), 7.84 (d, *J* = 7.8 Hz, 1H), 7.74 (brs, 2H), 7.57 (s, 2H), 5.42 (s, 2H). MS (ESI) *m/z* 512.2 ([M+H]⁺).

4.1.4. Procedures for synthesis of **11a–g** and **12a–g**

4.1.4.1. N-Cyclopropyl-4-((4-(3,5-dimethylisoxazol-4-yl)-1-oxophthalazin-2(1H)-yl)methyl)benzamide (**11a**). To stirred solution of **10a** (0.25 mmol) in 1,4-dioxane:H₂O (4:1, 10 mL) was added the 3,5-dimethylisoxazole-4-boronic acid (0.50 mmol), Pd(dppf)₂Cl₂ (0.005 mmol), Na₂CO₃ (4 mmol) under nitrogen, followed the mixture was refluxed for 36 h before being cooled to the room temperature. The reaction mixture was filtered and filtrate was evaporated in vacuo, the crude product was further purified by column chromatography on silica gel to yield compound **11a** (84%) as a white solid. m.p.: 184–186 °C. ¹H NMR (600 MHz, CDCl₃) δ 8.52 (d, *J* = 6.6 Hz, 1H), 7.84–7.80 (m, 2H), 7.70 (d, *J* = 8.4 Hz, 2H), 7.51 (d, *J* = 8.4 Hz, 2H), 7.43 (d, *J* = 6.6 Hz, 1H), 6.20 (s, 1H, NH), 5.47 (s, 2H), 2.89–2.87 (m, 1H), 2.31 (s, 3H), 2.15 (s, 3H), 0.88–0.84 (m, 2H), 0.62–0.57 (m, 2H). ¹³C NMR (150 MHz, CDCl₃) δ 168.3 (2C), 159.3, 158.9, 140.2, 138.1, 134.0, 133.4, 132.0, 129.5, 128.8 (2C), 128.3, 127.6, 127.1 (2C), 125.7, 111.1, 54.4, 23.1, 11.9, 10.6, 6.8 (2C). MS (ESI) 415.2 for [M+H]⁺.

4.1.4.2. N-Cyclopentyl-4-((4-(3,5-dimethylisoxazol-4-yl)-1-oxophthalazin-2(1H)-yl)methyl)benzamide (**11b**). With compound **10b**, a similar procedure as that described for **11a** gave pure **11b** (80%) as a white solid. m.p.: 194–196 °C. ¹H NMR (600 MHz, CDCl₃) δ 8.52 (d, *J* = 7.8 Hz, 1H), 7.84–7.78 (m, 2H), 7.71 (d, *J* = 7.8 Hz, 2H), 7.52 (d, *J* = 7.8 Hz, 2H), 7.43 (d, *J* = 7.8 Hz, 1H), 6.03 (d, *J* = 7.2 Hz,

1H, NH), 5.47 (s, 2H), 4.38 (q, $J = 6.6$ Hz, 1H), 2.31 (s, 3H), 2.15 (s, 3H), 2.11–2.04 (m, 2H), 1.73–1.62 (m, 4H), 1.50–1.43 (m, 2H). ^{13}C NMR (150 MHz, CDCl_3) δ 168.3, 166.6, 159.3, 158.8, 139.9, 138.0, 134.4, 133.4, 132.0, 129.4, 128.8 (2C), 128.2, 127.5, 127.1 (2C), 125.7, 111.0, 54.4, 51.7, 33.2 (2C), 23.8 (2C), 12.0, 10.7. MS (ESI) 443.2 for $[\text{M}+\text{H}]^+$.

4.1.4.3. *N*-Cyclohexyl-4-((4-(3,5-dimethylisoxazol-4-yl)-1-oxophthalazin-2(1H)-yl)methyl)benzamide (**11c**). With compound **10c**, a similar procedure as that described for **11a** gave pure **11c** (86%) as a white solid. m.p.: 198–200 °C. ^1H NMR (600 MHz, CDCl_3) δ 8.54–8.50 (m, 1H), 7.84–7.79 (m, 2H), 7.71 (d, $J = 7.2$ Hz, 2H), 7.52 (d, $J = 8.4$ Hz, 2H), 7.44–7.42 (m, 1H), 5.93 (d, $J = 7.8$ Hz, 1H, NH), 5.47 (s, 2H), 3.95 (t, $J = 3.6$ Hz, 1H), 2.32 (s, 3H), 2.16 (s, 3H), 2.00 (d, $J = 9.6$ Hz, 2H), 1.75–1.72 (m, 2H), 1.66–1.63 (m, 1H), 1.45–1.37 (m, 2H), 1.25–1.17 (m, 3H). ^{13}C NMR (150 MHz, CDCl_3) δ 168.3, 166.1, 159.3, 158.8, 139.8, 138.0, 134.5, 133.4, 132.0, 129.4, 128.8 (2C), 128.1, 127.5, 127.1 (2C), 125.7, 111.0, 54.5, 48.7, 33.2 (2C), 25.5, 24.8 (2C), 12.0, 10.7. MS (ESI) 457.2 for $[\text{M}+\text{H}]^+$.

4.1.4.4. 4-(3,5-Dimethylisoxazol-4-yl)-2-(4-(piperidine-1-carbonyl)benzyl)phthalazin-1(2H)-one (**11d**). With compound **10d**, a similar procedure as that described for **11a** gave pure **11d** (78%) as a white solid. m.p.: 188–190 °C. ^1H NMR (600 MHz, CDCl_3) δ 8.53 (d, $J = 7.8$ Hz, 1H), 7.84–7.79 (m, 2H), 7.50 (d, $J = 7.2$ Hz, 2H), 7.43 (t, $J = 7.8$ Hz, 1H), 7.35 (d, $J = 8.4$ Hz, 2H), 5.46 (s, 2H), 3.68 (brs, 2H), 3.30 (brs, 2H), 2.32 (s, 3H), 2.16 (s, 3H), 1.66 (s, 4H), 1.48 (s, 2H). ^{13}C NMR (150 MHz, CDCl_3) δ 169.9, 168.3, 159.4, 158.9, 137.9, 137.8, 136.1, 133.4, 132.0, 129.4, 128.8 (2C), 128.2, 127.6, 127.1 (2C), 125.7, 111.1, 54.5, 48.7, 43.1, 26.5, 25.6, 24.5, 12.0, 10.7. MS (ESI) 443.3 for $[\text{M}+\text{H}]^+$.

4.1.4.5. 4-(3,5-Dimethylisoxazol-4-yl)-2-(4-(morpholine-4-carbonyl)benzyl)phthalazin-1(2H)-one (**11e**). With compound **10e**, a similar procedure as that described for **11a** gave pure **11e** (79%) as a white solid. Yield 79%. m.p.: 137–139 °C. ^1H NMR (600 MHz, CDCl_3) δ 8.51 (d, $J = 6.0$ Hz, 1H), 7.83–7.78 (m, 2H), 7.52 (d, $J = 8.4$ Hz, 2H), 7.43 (d, $J = 8.4$ Hz, 1H), 7.36 (d, $J = 7.2$ Hz, 2H), 5.45 (s, 2H), 3.76–3.40 (m, 8H), 2.32 (s, 3H), 2.15 (s, 3H). ^{13}C NMR (150 MHz, CDCl_3) δ 169.7, 168.3, 159.3, 158.9, 138.5, 138.0, 134.8, 133.4, 132.0, 129.4, 128.9 (2C), 128.2, 127.5, 127.4 (2C), 125.7, 111.0, 66.8 (2C), 54.5, 48.6, 42.6, 12.0, 10.7. MS (ESI) 445.2 for $[\text{M}+\text{H}]^+$.

4.1.4.6. 4-((4-(3,5-Dimethylisoxazol-4-yl)-1-oxophthalazin-2(1H)-yl)methyl)-*N*-(1-methylpiperidin-4-yl)benzamide (**11f**). With compound **10f**, a similar procedure as that described for **11a** gave pure **11f** (75%) as a white solid. m.p.: 207–209 °C. ^1H NMR (600 MHz, $\text{DMSO}-d_6$) δ 8.46 (brs, 1H, NH), 8.37–8.35 (m, 1H), 7.93–7.90 (m, 2H), 7.82 (d, $J = 7.8$ Hz, 2H), 7.58–7.56 (m, 1H), 7.40 (d, $J = 7.8$ Hz, 2H), 5.42 (s, 2H), 3.96 (brs, 1H), 2.97 (brs, 2H), 2.64 (s, 3H), 2.30 (s, 3H), 2.07 (s, 3H), 1.94–1.84 (m, 4H), 1.22–1.18 (m, 2H). ^{13}C NMR (150 MHz, $\text{DMSO}-d_6$) δ 168.3, 165.6, 159.0, 158.1, 140.3, 137.4, 134.0, 133.5, 132.4, 128.9, 127.6 (2C), 127.5, 127.4, 126.6 (2C), 126.3, 110.6, 53.6, 52.5, 44.1, 42.4, 29.0, 28.6, 26.5, 11.6, 10.1. MS (ESI) 472.3 for $[\text{M}+\text{H}]^+$.

4.1.4.7. 4-((4-(3,5-Dimethylisoxazol-4-yl)-1-oxophthalazin-2(1H)-yl)methyl)-*N*-[(2,2,6,6-tetramethyl-1-oxyl)piperidin-4-yl]benzamide (**11g**). With compound **10g**, a similar procedure as that described for **11a** gave pure **11g** (78%) as a pink solid. m.p.: 164–166 °C. ^1H NMR (600 MHz, CDCl_3) (compound **11g** is a free-radical, some signals appear broadened and other signals are missing) δ 8.53 (brs, 1H), 7.84–7.74 (m, 3H), 7.59 (brs, 2H), 7.47 (brs, 1H), 7.18 (s, 1H), 5.49 (s, 2H), 2.33 (s, 3H), 2.16 (s, 3H). ^{13}C NMR (150 MHz, CDCl_3) δ 168.0, 166.5, 159.0, 158.6, 140.2, 137.8, 133.3, 131.9, 129.1,

128.9 (2C), 127.8, 127.5, 127.3, 125.5 (2C), 110.7, 54.2, 29.4, 11.9, 10.5. ESR (DMSO): $g = 2.007$. MS (ESI) 529.3 for $[\text{M}+\text{H}]^+$.

4.1.4.8. *N*-Cyclopropyl-4-((4-(1-methyl-1H-pyrazol-4-yl)-1-oxophthalazin-2(1H)-yl)methyl)benzamide (**12a**). With 1-methyl-4-(4,4,5,5-tetramethyl-1,3,2-dioxaborolan-2-yl)-1H-pyrazole, a similar procedure as that described for **11a** gave pure **12a** (86%) as a white solid. m.p.: 175–177 °C. ^1H NMR (600 MHz, CDCl_3) δ 8.50 (d, $J = 7.2$ Hz, 1H), 7.97 (d, $J = 7.2$ Hz, 1H), 7.83 (s, 1H), 7.82–7.77 (m, 2H), 7.72 (s, 1H), 7.68 (d, $J = 8.4$ Hz, 2H), 7.51 (d, $J = 8.4$ Hz, 1H), 6.25 (s, 1H, NH), 5.45 (s, 2H), 4.01 (s, 3H), 2.87 (q, $J = 3.6$ Hz, 1H), 0.87–0.81 (m, 2H), 0.61–0.57 (m, 2H). ^{13}C NMR (150 MHz, CDCl_3) δ 168.5, 158.9, 140.5, 140.3, 139.2, 133.8, 133.2, 131.5, 130.3, 129.3, 128.7 (2C), 128.2, 127.4, 127.1 (2C), 126.0, 117.0, 54.4, 39.2, 23.1, 6.8 (2C). MS (ESI) 400.2 for $[\text{M}+\text{H}]^+$.

4.1.4.9. *N*-Cyclopentyl-4-((4-(1-methyl-1H-pyrazol-4-yl)-1-oxophthalazin-2(1H)-yl)methyl)benzamide (**12b**). With compound **10b**, a similar procedure as that described for **12a** gave pure **12b** (88%) as a white solid. m.p.: 184–186 °C. ^1H NMR (600 MHz, CDCl_3) δ 8.51 (d, $J = 7.8$ Hz, 1H), 7.97 (d, $J = 7.2$ Hz, 1H), 7.83 (s, 1H), 7.82–7.77 (m, 2H), 7.73 (s, 1H), 7.70 (d, $J = 8.4$ Hz, 2H), 7.52 (d, $J = 8.4$ Hz, 2H), 6.04 (d, $J = 6.6$ Hz, 1H, NH), 5.46 (s, 2H), 4.37 (q, $J = 7.2$ Hz, 1H), 4.01 (s, 3H), 2.09–2.03 (m, 2H), 1.72–1.61 (m, 4H), 1.49–1.43 (m, 2H). ^{13}C NMR (150 MHz, CDCl_3) δ 166.8, 158.9, 140.3, 140.2, 139.2, 134.2, 133.2, 131.5, 130.3, 129.2, 128.7 (2C), 128.1, 127.4, 127.0 (2C), 125.9, 117.0, 54.4, 51.6, 39.2, 33.2 (2C), 23.7 (2C). MS (ESI) 428.2 for $[\text{M}+\text{H}]^+$.

4.1.4.10. *N*-Cyclohexyl-4-((4-(1-methyl-1H-pyrazol-4-yl)-1-oxophthalazin-2(1H)-yl)methyl)benzamide (**12c**). With compound **10c**, a similar procedure as that described for **12a** gave pure **12c** (90%) as a white solid. m.p.: 192–194 °C. ^1H NMR (600 MHz, CDCl_3) δ 8.51 (d, $J = 7.8$ Hz, 1H), 7.97 (d, $J = 7.8$ Hz, 1H), 7.83 (s, 1H), 7.81–7.77 (m, 2H), 7.73 (s, 1H), 7.70 (d, $J = 7.8$ Hz, 2H), 7.52 (d, $J = 7.8$ Hz, 2H), 5.91 (d, $J = 6.6$ Hz, 1H, NH), 5.46 (s, 2H), 4.01 (s, 3H), 3.96–3.94 (m, 1H), 1.99 (brs, 2H), 1.75–1.71 (m, 2H), 1.66–1.62 (m, 2H), 1.45–1.37 (m, 2H), 1.27–1.18 (m, 2H). ^{13}C NMR (150 MHz, CDCl_3) δ 166.3, 158.9, 140.3, 140.2, 140.1, 139.2, 134.4, 133.1, 130.3, 129.2, 128.7 (2C), 128.1, 127.4, 127.0 (2C), 125.9, 117.0, 54.5, 48.6, 39.2, 33.1, 25.5 (2C), 24.9, 24.8. MS (ESI) 442.2 for $[\text{M}+\text{H}]^+$.

4.1.4.11. 4-(1-Methyl-1H-pyrazol-4-yl)-2-(4-(piperidine-1-carbonyl)benzyl)phthalazin-1(2H)-one (**12d**). With compound **10d**, a similar procedure as that described for **12a** gave pure **12d** (82%) as a white solid. m.p.: 178–180 °C. ^1H NMR (600 MHz, CDCl_3) δ 8.52 (d, $J = 6.6$ Hz, 1H), 7.98 (d, $J = 7.8$ Hz, 1H), 7.84 (s, 1H), 7.83–7.79 (m, 2H), 7.75 (s, 1H), 7.51 (d, $J = 7.8$ Hz, 1H), 7.34 (d, $J = 7.8$ Hz, 2H), 5.45 (s, 2H), 4.02 (s, 3H), 3.68 (brs, 2H), 3.31 (brs, 2H), 1.65 (brs, 2H), 1.62 (brs, 2H), 1.47 (brs, 2H). ^{13}C NMR (150 MHz, CDCl_3) δ 170.0, 158.9, 140.2, 139.2, 138.2, 135.8, 133.1, 131.5, 130.3, 129.3, 128.6 (2C), 128.2, 127.4, 127.1 (2C), 125.9, 117.1, 54.5, 48.7, 43.1, 39.2, 26.5, 25.6, 24.6. MS (ESI) 428.3 for $[\text{M}+\text{H}]^+$.

4.1.4.12. 4-(1-Methyl-1H-pyrazol-4-yl)-2-(4-(morpholine-4-carbonyl)benzyl)phthalazin-1(2H)-one (**12e**). With compound **10e**, a similar procedure as that described for **12a** gave pure **12e** (81%) as a white solid. m.p.: 170–172 °C. ^1H NMR (600 MHz, CDCl_3) δ 8.51 (d, $J = 9.0$ Hz, 1H), 7.98 (d, $J = 7.8$ Hz, 1H), 7.85 (s, 1H), 7.80–7.78 (m, 2H), 7.75 (s, 1H), 7.53 (d, $J = 7.8$ Hz, 2H), 7.36 (d, $J = 8.4$ Hz, 2H), 5.45 (s, 2H), 4.02 (s, 3H), 3.74–3.40 (m, 8H). ^{13}C NMR (150 MHz, CDCl_3) δ 170.2, 158.9, 140.2, 139.2, 138.8, 134.6, 133.2, 131.5, 130.3, 129.3, 128.7 (2C), 128.2, 127.4 (3C), 125.9, 117.0, 66.8 (2C), 54.6, 48.2, 42.7, 39.3. MS (ESI) 430.2 for $[\text{M}+\text{H}]^+$.

4.1.4.13. 4-((4-(1-Methyl-1H-pyrazol-4-yl)-1-oxophthalazin-2(1H)-yl)methyl)-N-(1-methylpiperidin-4-yl)benzamide (**12f**). With compound **10f**, a similar procedure as that described for **12a** gave pure **12f** (80%) as a white solid. m.p.: 200–202 °C. ¹H NMR (600 MHz, DMSO *d*₆) δ 8.37 (d, *J* = 6.6 Hz, 1H), 8.25 (d, *J* = 7.2 Hz, 1H), 8.24 (s, 1H), 8.09 (d, *J* = 7.8 Hz, 1H), 7.99–7.90 (m, 2H), 7.83 (s, 1H), 7.80 (d, *J* = 8.4 Hz, 2H), 7.42 (d, *J* = 8.4 Hz, 2H), 5.40 (s, 2H), 3.94 (s, 3H), 3.78–3.74 (m, 1H), 2.86 (d, *J* = 11.4 Hz, 2H), 2.25 (s, 3H), 2.14 (brs, 2H), 1.77 (d, *J* = 10.8 Hz, 2H), 1.66–1.58 (m, 2H). ¹³C NMR (150 MHz, DMSO *d*₆) δ 172.4, 165.5, 157.9, 140.2, 139.8, 138.5, 133.8, 132.0, 131.2, 128.5 (3C), 127.5, 127.4, 126.6 (2C), 126.3, 115.8, 53.9, 53.6, 45.9, 45.2, 38.7, 30.8 (2C), 21.2. MS (ESI) 457.3 for [M+H]⁺.

4.1.4.14. 4-((4-(1-Methyl-1H-pyrazol-4-yl)-1-oxophthalazin-2(1H)-yl)methyl)-N-[(2,2,6,6-tetramethyl-1-oxyl)piperidin-4-yl]benzamide (**12g**). With compound **10g**, a similar procedure as that described for **12a** gave pure **12g** (84%) as a pink solid. m.p.: 150–152 °C. ¹H NMR (600 MHz, DMSO *d*₆) (compound **12g** is a free-radical, some signals appear broadened and other signals are missing) δ 8.52 (brs, 1H), 7.99 (s, 1H), 7.85–7.74 (m, 5H), 7.58 (s, 2H), 7.19 (s, 1H), 5.48 (s, 2H), 4.03 (s, 3H), 2.16 (s, 3H). ¹³C NMR (150 MHz, CDCl₃) δ 165.6, 157.5, 139.4, 138.9, 137.9, 131.9, 130.3, 129.1, 127.9, 127.6 (2C), 126.8, 126.2, 126.1, 124.6 (2C), 115.6, 53.2, 38.1, 23.6. ESR (DMSO): *g* = 2.007. MS (ESI) 514.3 for [M+H]⁺.

4.1.5. Procedures for synthesis of **13a-c**

4.1.5.1. *N*-Cyclohexyl-4-((4-(1-methyl-1H-pyrazol-4-yl)amino)-1-oxophthalazin-2(1H)-yl)methylbenzamide (**13a**). To stirred solution of **10c** (0.2 mmol) in dry toluene (8 mL) was added the 1-methyl-1H-pyrazol-4-amine (0.28 mmol), *t*-BuOK (0.28 mmol), 2-(di-*tert*-butylphosphino)biphenyl (0.02 mmol) and Pd₂dba₃ (0.01 mmol) under nitrogen, followed the mixture was refluxed for 36 h before being cooled to the room temperature. The reaction mixture was filtered and filtrate was evaporated in vacuo, the crude product was further purified by column chromatography on silica gel to yield compound **13a** (67%) as a white solid. m.p.: 234–236 °C. ¹H NMR (600 MHz, DMSO *d*₆) δ 8.98 (s, 1H), 8.30 (t, *J* = 6.6 Hz, 2H), 8.11 (d, *J* = 7.8 Hz, 1H), 7.95 (t, *J* = 7.2 Hz, 1H), 7.85 (t, *J* = 7.2 Hz, 1H), 7.79 (d, *J* = 7.8 Hz, 2H), 7.71 (s, 1H), 7.50–7.44 (m, 3H), 5.30 (s, 2H), 3.77–3.75 (m, 4H), 1.76 (brs, 2H), 1.68 (brs, 2H), 1.57 (d, *J* = 12.0 Hz, 1H), 1.30–1.20 (m, 4H), 1.09 (brs, 1H). ¹³C NMR (150 MHz, DMSO *d*₆) δ 165.1, 156.5, 140.8, 140.7, 133.9, 133.0, 131.6, 129.7, 128.0 (2C), 127.9, 127.4 (2C), 127.0, 124.3, 123.4, 122.8, 120.4, 52.6, 48.2, 38.6, 32.3 (2C), 25.2, 24.9 (2C). MS (ESI) 457.3 for [M+H]⁺.

4.1.5.2. *N*-Cyclohexyl-4-((4-(4-(morpholine-4-carbonyl)phenyl)amino)-1-oxophthalazin-2(1H)-yl)methylbenzamide (**13b**). With compound **6a**, a similar procedure as that described for **13a** gave pure **13b** (81%) as a white solid. m.p.: 152–154 °C. ¹H NMR (600 MHz, CDCl₃) δ 8.51–8.48 (m, 1H), 7.84 (t, *J* = 4.2 Hz, 1H), 7.76 (t, *J* = 4.2 Hz, 2H), 7.68 (d, *J* = 8.4 Hz, 2H), 7.46 (d, *J* = 7.8 Hz, 2H), 7.35 (d, *J* = 8.4 Hz, 2H), 7.30 (d, *J* = 8.4 Hz, 2H), 6.97 (s, 1H), 6.10 (d, *J* = 8.4 Hz, 1H), 5.33 (s, 2H), 3.93 (t, *J* = 4.2 Hz, 1H), 3.80–3.50 (m, 8H), 1.98 (d, *J* = 10.2 Hz, 2H), 1.74–1.71 (m, 3H), 1.62 (d, *J* = 13.2 Hz, 1H), 1.42–1.34 (m, 2H), 1.25–1.15 (m, 4H). ¹³C NMR (150 MHz, CDCl₃) δ 170.3, 166.3, 157.9, 142.4, 140.9, 140.4, 134.5, 132.9, 131.7, 128.8 (2C), 128.5 (2C), 128.1, 128.0, 127.1 (2C), 125.2, 121.9, 118.2 (2C), 66.9 (2C), 53.7, 48.7, 33.1 (2C), 29.7 (2C), 25.5, 24.9 (2C). MS (ESI) 566.3 for [M+H]⁺.

4.1.5.3. *N*-(2-Chlorophenyl)-4-((3-(4-(cyclohexylcarbamoyl)benzyl)-4-oxo-3,4-dihydrophthalazin-1-yl)amino)benzamide (**13c**). With compound **6c**, a similar procedure as that described for **13a** gave pure **13c** (87%) as a white solid. m.p.: 277–279 °C. ¹H NMR (600

MHz, DMSO *d*₆) δ 9.77 (s, 1H), 9.09 (s, 1H), 8.39 (d, *J* = 8.4 Hz, 1H), 8.36 (d, *J* = 8.4 Hz, 1H), 8.12 (d, *J* = 7.8 Hz, 1H), 8.02 (t, *J* = 7.2 Hz, 1H), 7.92 (t, *J* = 7.2 Hz, 1H), 7.88 (d, *J* = 9.0 Hz, 2H), 7.81 (d, *J* = 8.4 Hz, 2H), 7.67 (d, *J* = 9.0 Hz, 2H), 7.61 (d, *J* = 8.4 Hz, 1H), 7.53 (dd, *J* = 7.8, 1.2 Hz, 1H), 7.45 (d, *J* = 7.8 Hz, 2H), 7.36 (td, *J* = 7.8, 1.2 Hz, 1H), 7.26 (td, *J* = 7.8, 1.2 Hz, 1H), 5.32 (s, 2H), 3.70 (t, *J* = 3.6 Hz, 1H), 1.77 (d, *J* = 7.2 Hz, 2H), 1.67 (d, *J* = 4.8 Hz, 2H), 1.55 (d, *J* = 11.4 Hz, 1H), 1.29–1.20 (m, 4H), 1.08–1.05 (m, 1H). ¹³C NMR (150 MHz, DMSO *d*₆) δ 165.1, 164.8, 156.9, 144.6, 140.9, 140.4, 135.3, 134.1, 133.2, 132.1, 129.4, 129.1, 128.5, 128.1, 127.9 (2C), 127.5 (2C), 127.4 (2C), 127.0 (2C), 126.9, 125.8, 124.9, 123.6, 117.6 (2C), 52.7, 48.3, 32.3 (2C), 25.2, 24.9 (2C). MS (ESI) 606.3 for [M+H]⁺.

4.2. Biology

4.2.1. Cell lines and culture conditions

HeLa (human cervical carcinoma cell line), A549 (human lung cancer cell line), HepG2 (human hepatoma cell line), LoVo (human colonic carcinoma cell line) and HCT-116 (human colonic carcinoma cell line) were provided by General Hospital of Lanzhou Military Command. The cell was routinely cultured in RPMI-1640 medium, supplemented with 10% fetal bovine serum (FBS). The culture was maintained at 37 °C with a gas mixture of 5% CO₂/95% air. All media were supplemented with 5 mg/mL penicillin and 5 mg/mL streptomycin.

4.2.2. Antiproliferation activities assays

Cells were incubated at 37 °C in a 5% CO₂ atmosphere. The MTT assay were used to determined growth inhibition. The HeLa, A-549, HepG2, LoVo and HCT-116 cells were seeded in 96-well plates at a density of 5 × 10³ cells/well in 150 μL of the medium with 10% heat-inactivated NBS for 24 h. The synthetic compounds **11a-g**, **12a-g**, **13a-c** and reference compound **1** and VX-680 were dissolved to five concentrations (0.01, 0.1, 1, 10 and 100 μM) in the medium and then added them to the well and incubated at 37 °C for 72 h, then the media was aspirated, and 10 μL of 5 mg/mL MTT solution (diluted in sterile PBS) diluted in serum-free media was added to each well. 4 h later, the supernatant was discarded and 100 μL of DMSO was added to each well. The mixture was shaken on an oscillator and measured at 490 nm using universal microplate reader (Infinite M200 Pro, Tecan Inc.). IC₅₀ values were determined from a log plot of percent of control versus concentration.

4.2.3. Aurora kinase assays

The synthetic compounds and reference compound were diluted to five concentrations (0.1, 1, 10, 100 and 1000 nM) in the PBS and then added 5 μL to the 50 μL reaction mixture (40 mM Tris, pH = 7.4, 10 mM MgCl₂, 1 mM DTT, 0.1 mg/ml BSA, 10 μM ATP, 0.2 μg/ml Kinase and 100 μM Kemptide acetate salt), and then the kinase reactions were incubated for 30 min at 37 °C. Finally, we used Kinase-Glo luminescence kinase assay kit tested luminescent signal of the reaction mixture, gave IC₅₀ values by GraphPad Prism software.

4.2.4. Western blotting analysis

HeLa cells were treated with **12c** (0, 0.5, 2.0 and 5.0 μM) or VX-680 (5.0 μM) for 6 or 24 h. For total cell protein extracts, cells were washed and lysed in lysis buffer (50 mM Tris-HCl (pH 7.5), 1% NP-40, 2 mM EDTA, 10 mM NaCl, 10 μg/ml Aprotinin, 10 μg/ml Leupeptin, 1 mM DTT, 0.1% SDS and 1 mM phenyl methyl sulfonyl fluoride). Total proteins were achieved by centrifuging (12,000g for 20 min at 4 °C). The protein concentrations were determined by using BCA protein assay kit (Beyotime, Jiangsu, China). For western blot analysis, equal amounts of proteins (20–30 μg) were

separated on 12% SDS-PAGE gels and transferred to polyvinylidene difluoride (PVDF) membranes (Millipore Corporation, USA). The blot was blocked in blocking buffer (5% non-fat dry milk in TBST) for 2 h at room temperature, and then incubated with dilute solution (1:500–1:1000) of the antibody against AurA and AurB (Abcam), the antibody against phospho-AurA (Thr288) and phospho-AurB (Thr232) (Cell Signaling Technology), the antibodies against cyclinB1 and cdc2 (BioLegend) and the antibody against β -actin (ZSGB-BIO) in blocking buffer overnight at 4 °C. The blot was then incubated with appropriate secondary antibody (1:5000–1:10000 dilution), β -Actin was used as a loading control. The protein bands were visualized using the Gel Imaging System (ChemDoc-It610, UVP, USA).

4.2.5. Analysis of cell cycle by flow cytometry

The cell cycle was analyzed by flow cytometry. Firstly, HeLa cells were treated with different concentrations of compound **12c** (0, 0.5, 2.0 and 5.0 μ M) or VX-680 (5.0 μ M) for 24 h. After incubation, a total of $(1-5) \times 10^5$ cells were harvested from the treated and normal samples. The cells were washed twice with PBS and fixed in 75% ice-cold ethanol for at least overnight. The sample was concentrated by removing the ethanol and then cells were then washed three times with PBS, staining the cellular DNA with fluorescent solution (1% (v/v) Triton X-100, 0.01% RNase, 0.05% PI) for 15 min in darkness. The cell cycle distribution was then detected by flow cytometry (COULTER EPICS XL, USA). All experiments were performed three times.

4.3. Molecular docking

The crystal structures of AurA (PDB code: 3D14) and AurB (PDB code: 4C2V) were derived from the PDB database, and then AurA (or AurB) and the compound **12c** were performed docking using the Glide module of Schrödinger software. Firstly, AurA (or AurB) and the compound **12c** were adopted optimization. Next, the binding sites of the protein and the compound **12c** were defined. Finally, molecular docking was performed. In the docking process, we used a semi-flexible docking, the compound **12c** was docked to the appropriate combination pockets of protein, and finally we chose the best combination model.

Acknowledgments

We gratefully acknowledge the financial support from the National Natural Science Foundation of China (No. 21672093 and 21372110).

A. Supplementary data

Supplementary data associated with this article can be found, in the online version, at <https://doi.org/10.1016/j.bmc.2018.04.048>.

References

- Li JJ, Li SA. Mitotic kinases: the key to duplication, segregation, and cytokinesis errors, chromosomal instability, and oncogenesis. *Pharmacol Ther.* 2006;111:974–984.
- Carmena M, Earnshaw WC. The cellular geography of aurora kinases. *Nat Rev Mol Cell Biol.* 2003;4:842–854.
- Katayama H, Brinkley WR, Sen S. The aurora kinases: role in cell transformation and tumorigenesis. *Cancer Metastasis Rev.* 2003;22:451–464.
- Glover DM, Leibowitz MH, Mclean DA, Parry H. Mutations in Aurora prevent centrosome separation leading to the formation of monopolar spindles. *Cell.* 1995;81:95–105.
- Nigg EA. Mitotic kinases as regulators of cell division and its checkpoints. *Nat Rev Mol Cell Biol.* 2001;2:21–32.
- Kilchmann F, Marcaida MJ, Kotak S, et al. Discovery of a selective aurora A kinase inhibitor by virtual screening. *J Med Chem.* 2016;59:7188–7211.
- Fu J, Bian M, Jiang Q, Zhang C. Roles of Aurora kinases in mitosis and tumorigenesis. *Mol Cancer Res.* 2007;5:1–10.
- Vader G, Lens SM. The Aurora kinase family in cell division and cancer. *Bioch Biophys Acta.* 2008;1786:60–72.
- Linardopoulos S, Blagg J. Aurora kinase inhibition: a new light in the sky? *J Med Chem.* 2015;58:5186–5188.
- Barr AR, Gergely F. Aurora-A: the maker and breaker of spindle poles. *Cell Sci.* 2007;120:2987–2996.
- Saeki T, Ouchi M, Ouchi T. Physiological and oncogenic Aurora – a pathway. *Int J Biol Sci.* 2009;5:758–762.
- Vader G, Lens MSMA. The chromosomal passenger complex: guiding Aurora-B through mitosis. *J Cell Biol.* 2006;173:833–837.
- Sasai K, Katayama H, Stenoien DL, et al. Aurora-C kinase is a novel chromosomal passenger protein that can complement Aurora-B kinase function in mitotic cells. *Cell Motil Cytoskelet.* 2004;59:249–263.
- Borisa AC, Bhatt HG. A comprehensive review on Aurora kinase: small molecule inhibitors and clinical trial studies. *Eur J Med Chem.* 2017;140:1–19.
- Harrington EA, Bebbington D, Moore J, et al. VX-680, a potent and selective small-molecule inhibitor of the Aurora kinases, suppresses tumor growth in vivo. *Nat Med.* 2004;10:262–267.
- Pollard JR, Mortimore M. Discovery and development of aurora kinase inhibitors as anticancer agents. *J Med Chem.* 2009;52:2629–2651.
- Howard S, Berdini V, Boulstridge JA, et al. Fragment-Based discovery of the pyrazol-4-yl urea (AT9283), a multitargeted kinase inhibitor with potent Aurora kinase activity. *J Med Chem.* 2009;52:379–388.
- Yang J, Ikezoe T, Nishioka C, et al. AZD1152, a novel and selective aurora B kinase inhibitor, induces growth arrest, apoptosis, and sensitization for tubulin depolymerizing agent or topoisoemerase II inhibitor in human acute leukemia cells in vitro and in vivo. *Blood.* 2007;110:2034–2040.
- Payton M, Bush TL, Chung G, et al. Preclinical evaluation of AMG 900, a novel potent and highly selective pan-aurora kinase inhibitor with activity in taxane-resistant tumor cell lines. *Cancer Res.* 2010;70:9846–9854.
- Demirayak S, Karaburun AC, Beis R. Some pyrrole substituted aryl pyridazinone and phthalazinone derivatives and their antihypertensive activities. *Eur J Med Chem.* 2004;39:1089–1095.
- Mood AD, Premachandre IDUA, Hiew S, et al. Potent antifungal synergy of phthalazinone and isoquinolones with azoles against *Candida albicans*. *ACS Med Chem Lett.* 2017;8:168–173.
- Procopiou PA, Ford AJ, Gore PM, et al. Design of phthalazinone amide Histamine H1 receptor antagonists for use in rhinitis. *ACS Med Chem Lett.* 2017;8:577–581.
- Biswas K, Peterkin TAN, Bryan MC, et al. Discovery of potent, orally bioavailable phthalazinone bradykinin B1 receptor antagonists. *J Med Chem.* 2011;54:7232–7246.
- Prime ME, Courtney SM, Brookfield FA, et al. Phthalazinone pyrazoles as potent, selective, and orally bioavailable inhibitors of Aurora-A kinase. *J Med Chem.* 2011;54:312–319.
- Qin WW, Sang CY, Zhang LL, et al. Synthesis and biological evaluation of 2,4-diaminopyrimidines as selective Aurora A kinase inhibitors. *Eur J Med Chem.* 2015;95:174–184.
- Zhao J, Guan XW, Chen SW, Hui L. Synthesis and biological evaluation of norcantharidin derivatives as protein phosphatase-1 inhibitors. *Bioorg Med Chem Lett.* 2015;25:363–366.
- Christensen H, Søren Kil A, Damjohansen K, et al. Effect of solvents on the product distribution and reaction rate of a Buchwald–Hartwig amination reaction. *Org Process Res Dev.* 2006;10:762–769.
- Huang WT, Liu J, Liu JF, et al. Synthesis and biological evaluation of conjugates of deoxydophyllotoxin and 5-FU as inducer of caspase-3 and -7. *Eur J Med Chem.* 2012;49:48–54.
- Kashem MA, Nelson RM, Yingling JD, et al. Three mechanistically distinct kinase assays compared: measurement of intrinsic ATPase activity identified the most comprehensive set of ITK inhibitors. *J Biomol Screen.* 2007;12:70–83.
- Bayliss R, Sardon T, Vernos I, Conti E. Structural basis of Aurora-A activation by TPX2 at the mitotic spindle. *Mol Cell.* 2003;12:851–862.
- Li Y, Zhou WQ, Wei LL, et al. The effect of Aurora kinases on cell proliferation, cell cycle regulation and metastasis in renal cell carcinoma. *Int J Oncol.* 2012;41:2139–2149.
- Giet R, Prigent C. The non-catalytic domain of the *Xenopus laevis* auroraA kinase localises the protein to the centrosome. *J Cell Sci.* 2011;114:2095–2104.
- Guan XW, Xu XH, Feng SL, et al. Synthesis of hybrid 4-deoxydophyllotoxin-5-fluorouracil compounds that inhibit cellular migration and induce cell cycle arrest. *Bioorg Med Chem Lett.* 2016;26:1561–1566.
- Hailt MM, Ebrahim HY, Mohyeldin MM, et al. The tobacco cembranoid (1S,2E,4S,7E,11E)-2,7,11-cembratriene-4,6-diol as a novel angiogenesis inhibitory lead for the control of breast malignancies. *Bioorg Med Chem.* 2017;25:3911–3921.
- DeLano L. *The PyMOL molecular graphics system*. Palo Alto, CA, USA: DeLano Scientific; 2002.
- Cheng C, Liu ZG, Zhang H, et al. Enhancing chemosensitivity in ABCB1- and ABCG2-overexpressing cells and cancer stem-like cells by an Aurora kinase inhibitor CCT129202. *Mol Pharm.* 2012;9:1971–1982.
- Nar A, Ozen O, Tutuncu NB, Demirhan B. Cyclin A and cyclin B1 overexpression in differentiated thyroid carcinoma. *Med Oncol.* 2012;29:294–300.
- Liu JF, Sang CY, Qin WW, et al. Synthesis and evaluation of the cell cycle arrest and CT DNA interaction properties of 4b-amino-40-O-demethyl-4-deoxydophyllotoxins. *Bioorg Med Chem.* 2013;21:6948–6955.